

Predictions on high frequency polarization properties of extragalactic radio sources and implications for CMB polarization measurements

M. Tucci,¹ E. Martínez–González,¹ L. Toffolatti,² J. González–Nuevo² and G. De Zotti³

¹ *Instituto de Física de Cantabria, Consejo Superior de Investigaciones Científicas – Universidad Cantabria, Avda. Los Castros s/n, 39005 Santander, Spain*

² *Departamento de Física, Universidad de Oviedo, c/ Calvo Sotelo s/n, 33007 Oviedo, Spain*

³ *Osservatorio Astronomico di Padova, INAF, Vicoletto dell’Osservatorio 5, I-35122 Padova, Italy*

4 November 2018

ABSTRACT

We present a method to simulate the polarization properties of extragalactic radio sources at microwave frequencies. Polarization measurements of nearly 2×10^6 sources at 1.4 GHz are provided by the NVSS survey. Using this catalogue and the GB6 survey, we study the distribution of the polarization degree of both steep– and flat–spectrum sources. We find that the polarization degree is anti–correlated with the flux density for the former population, while no correlation is detected for the latter. The available high–frequency data are exploited to determine the frequency dependence of the distribution of polarization degrees. Using such information and the evolutionary model by Toffolatti et al. (1998), we estimate the polarization power spectrum of extragalactic radio sources at ≥ 30 GHz and their contamination of CMB polarization maps. Two distinct methods to compute point–source polarization spectra are presented, extending and improving the one generally used in previous analyses. While extragalactic radio sources can significantly contaminate the CMB E-mode power spectrum only at low frequencies ($\nu \lesssim 30$ GHz), they can severely constrain the detectability of the CMB B-mode up to $\nu \simeq 100$ GHz.

Key words: radio continuum: galaxies – polarization – cosmic microwave background

1 INTRODUCTION

In the last year, two experiments provided the first observational evidence of the polarization of the Cosmic Microwave Background (CMB) radiation: DASI (Kovac et al. 2002) achieved a direct measure of E–mode polarization (see Kamionkowski et al. 1997 and Zaldarriaga & Seljak 1997 for a definition of E and B modes), while WMAP (Bennett et al. 2003a) detected the cross–correlation between the CMB temperature anisotropies and E–mode polarization, giving an estimate of the reionization optical depth (Kogut et al. 2003). A large number of experiments have been planned to measure the CMB polarization (see Cecchini et al. 2002; Hanany & Olive 2003), motivated by its huge information content. Besides probing the ionization history, the CMB polarization can open a window on the primordial phase of the Universe through the detection of the B–mode, i.e. the curl component of the polarization field. In fact, the B–mode po-

larization is generated by tensor metric perturbations and, in inflation models, its amplitude is directly proportional to the energy scale at which the inflation has occurred. However, the detection of this component is a real challenge, not only due to the very low level of the signal, but also to the presence of foregrounds and effects that can mix the E– and B–modes of the CMB polarization. For example, the gravitational lensing produced by large scale structures converts a fraction of the CMB E–mode component to the B–mode one. Although the effect is of a few percent or below, the lensing–induced curl mode can overwhelm the primordial one (Zaldarriaga & Seljak 1998; Knox & Song 2002).

Our knowledge of foreground polarization is still poor. Among the Galactic emissions which dominate foreground intensity fluctuations on large angular scales, free–free is nearly unpolarized while synchrotron is highly polarized; its polarization properties have been studied at GHz frequencies (Tucci et al. 2000, 2002; Baccigalupi et al. 2001;

Bruscoli et al. 2002), but we have little or no direct information at frequencies of interest for CMB studies. At mm wavelengths, the Galactic polarized signal is due essentially to the dust emission. Estimates of this contribution have been so far provided only by models based on HI maps (Prunet et al. 1998) or on the starlight polarization (Fosalba et al. 2002), although direct sub-mm measurements over a substantial fraction of the sky have been recently provided by the ARCHEOPS experiment (Benoit et al. 2003).

In this paper we deal with extragalactic radio sources, which are expected to be the dominant polarized foreground on small angular scales. Accurate studies of their contribution to intensity fluctuations, based on evolutionary models fitting the available data at many frequencies, have been published. In our analysis we adopt the Toffolatti et al. (1998) (hereafter T98) model in order to predict the number counts of extragalactic radio sources at cm and mm wavelengths. This model reproduces very well the number counts of different classes of bright radio sources at GHz frequencies (see Sections 2 and 3); moreover, the accuracy of its high-frequencies predictions has been confirmed by the recent VSA (Taylor et al. 2001; Waldram et al. 2003), CBI (Mason et al. 2003) and WMAP (Bennett et al. 2003b) surveys between 15 and 44 GHz (Toffolatti et al. 2003). More specifically, the WMAP survey has detected 208 sources in a sky area of 10.38 sr at $|\delta^{II}| > 10^\circ$ at flux densities $S \geq 0.9$ –1.0 Jy. The T98 model predicts 270–280 sources in the same sky area, so that the average offset is a factor of ~ 0.75 . Moreover the distribution of spectral indexes in the WMAP sample peaks around $\alpha = 0.0$, which is exactly the mean spectral index for flat-spectrum sources adopted by T98, and the fraction of steep-spectrum (i.e., $\alpha > 0.5$, $S \propto \nu^{-\alpha}$) sources is of $\sim 12\%$, to be compared with a predicted fraction of $\simeq 10\%$. As a curiosity, we also note that the brightest source detected by WMAP has a flux density of $S \simeq 25$ Jy which corresponds exactly to the value for which the model predicts 1 source all over the sky.

Most of the available information on polarization properties of extragalactic sources refers to GHz frequencies, while for CMB studies we are interested in frequencies $\gtrsim 30$ GHz. There are at least two reasons to expect polarization properties to be frequency dependent, and, in particular, higher polarization at higher frequencies. First, at low frequencies substantial depolarization may be induced by Faraday rotation. Determinations of rotation measures for radio galaxies and quasars yield values from tens to 10^3 rad m^{-2} (O'Dea 1989; Taylor 2000; Pentericci et al. 2000; Mesa et al. 2002, henceforth M02), implying that depolarization may be significant up to $\nu \simeq 10$ GHz. Second, especially in compact objects, as the observing frequencies increase emitting regions are closer and closer to the nucleus, where the degree of the ordering of magnetic fields and, as a consequence, the polarization degree, may be higher and higher.

Preliminary estimates of the contribution of extragalactic radio sources to the polarization angular power spectrum (APS) were worked out by De Zotti et al. (1999) and M02. De Zotti et al. (1999) simply scaled the temperature power spectrum by the mean squared polarization degree of radio sources, assuming a Poisson spatial distribution. M02, instead, computed the APS directly from the NVSS polarimetric data (Condon et al. 1998), estimating a factor of 3 increase in the polarization degree of steep-spectrum sources

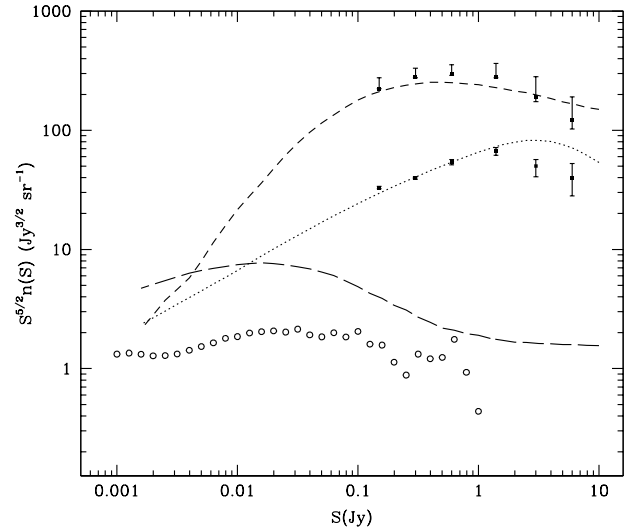


Figure 1. Differential number counts, normalized to $S^{5/2}$, of steep- (upper data points) and flat-spectrum (lower data points) NVSS sources, compared with predictions of the T98 model (steep-spectrum sources: short dashed curve; flat-spectrum sources: dotted curve; “starburst” galaxies: long dashed curve). The upper part of error bars for steep spectrum sources allows for the possibility that NVSS sources missing a GB6 counterpart belong to this population. The dots show the total differential counts in terms of polarized flux.

from 1.4 GHz to ≥ 20 GHz and assuming that, for flat-spectrum sources, the polarization degree either is frequency independent or increases by a factor of 3.

In this paper, we improve on previous estimates by studying the probability distribution of the polarization degree for both steep- and flat-spectrum sources at $\nu \leq 15$ GHz, providing a recipe to extrapolate the distributions to higher frequencies. Our results consist of a technique to generate simulated catalogues of extragalactic radio sources and also in accurate expressions to estimate the polarization APS, after having removed the strongest polarized sources.

2 POLARIZATION PROPERTIES OF NVSS SOURCES

The starting point of the analysis is the NRAO VLA Sky Survey (NVSS; Condon et al. 1998). This survey covers $\Omega \simeq 10.3 \text{ sr}$ of the sky with $\delta \geq -40^\circ$ at 1.4 GHz, providing the flux density S and the Stokes parameters Q and U of almost 2×10^6 discrete sources with $S \gtrsim 2.5 \text{ mJy}$. The images obtained from interferometric data have $\theta = 45'' \text{ FWHM}$ resolution and the rms brightness fluctuation in the Q and U parameters is $\sigma \simeq 0.29 \text{ mJy beam}^{-1}$.

Information on the spectral index α of NVSS sources is obtained exploiting the Green Bank 4.85 GHz survey (GB6, Gregory et al. 1996), which covers the declinations $0^\circ < \delta < 75^\circ$ ($\Omega \simeq 6.07 \text{ sr}$) to a flux limit of $S_{4.85} = 18 \text{ mJy}$ with a resolution FWHM = 3.5 arcmin. We have cross-matched the positions of NVSS sources with $S_{1.4} \geq 100 \text{ mJy}$ with the

Table 1. Polarization degree at 1.4 GHz of steep- and flat-spectrum sources.

flux(mJy)	flat					steep				
	N	N(T98)	N _{Π<1%} (%)	median(%)	mean(%)	N	N(T98)	N _{Π<1%} (%)	median(%)	mean(%)
100–200	2305	2144	43.3	1.33	2.16	15621	15409	35.8	1.77	2.70
200–400	980	1045	43.5	1.24	2.01	6925	6006	40.0	1.52	2.40
400–800	473	486	40.2	1.50	1.95	2552	2428	41.2	1.44	2.25
> 800	260	364	45.7	1.12	1.92	1096	1165	47.0	1.14	2.02

GB6 catalogue, taking all matches with position offsets less than 3 times the uncertainty on the GB6 position. Sources with Galactic latitude $|b| \leq 2^\circ$ have been rejected, in order to guarantee that nearly all the sources are extragalactic. The 100 mJy flux limit has been chosen to have $\gtrsim 3\sigma$ detections of polarization down to a percent level. About 86% of NVSS sources turned out to have a GB6 counterpart. Whenever more than one NVSS source falls within the GB6 beam, as a consequence of the better NVSS angular resolution which may lead to individually resolve multiple components, we have summed up their fluxes, corrected for the effect of the GB6 beam. We ended up with a sub-sample of 29299 NVSS sources, of which $\sim 87\%$ are steep-spectrum ($\alpha > 0.5$) and $\sim 13\%$ are flat-spectrum ($\alpha \leq 0.5$).

In Fig. 1 we show the differential number counts of NVSS sources as a function of the total and linearly polarized ($PI = \sqrt{Q^2 + U^2}$) flux density. The predictions of the T98 model (for a flat CDM cosmology with $\Omega_\Lambda = 0.7$ and $h = 0.7$) are also displayed. According to the model, the dominant contribution at high and moderate fluxes comes from steep-spectrum sources, while “starburst” galaxies are negligible for S above a few tens of mJy. The fraction of flat-spectrum sources increases with flux density and is important at the Jy level. As shown by Table 1 and by Fig. 1, the observed number of flat- and steep-spectrum sources in total flux-density bins compares favourably with the predictions, $N(T98)$, of the T98 model. The latter only weakly overestimates the observed number of flat-spectrum sources for $S > 800$ mJy; such discrepancy will be taken into account when computing their contribution to the polarization power spectrum in Section 5.

It is interesting to note that the normalized PI number counts keep nearly constant over all the flux density range where they are defined. The different shape compared with the total power number counts indicates a dependence of the polarization degree on flux density (see below).

Following the analysis of M02, we study the distribution of the percentage polarization degree ($\Pi = 100PI/S$) at 1.4 GHz for steep- and flat-spectrum sources for different flux-density intervals (see Figs. 2 and 3). Table 1 reports the median and the mean value of Π for such distributions and the percentage of sources with Π lower than 1% ($N_{\Pi<1\%}$). The low- Π tail of distributions is contaminated by noise and residual instrumental polarization; however, while the relevance of the noise decreases when the polarized intensity increases, the latter is proportional to the flux density of sources. Condon et al. (1998) found that the instrumental polarization is $\approx 0.12\%$ of S for a large sample of sources stronger than 1 Jy and estimated that, in any case, it should be less than 0.3%.

The results of Table 1 highlight an anti-correlation be-

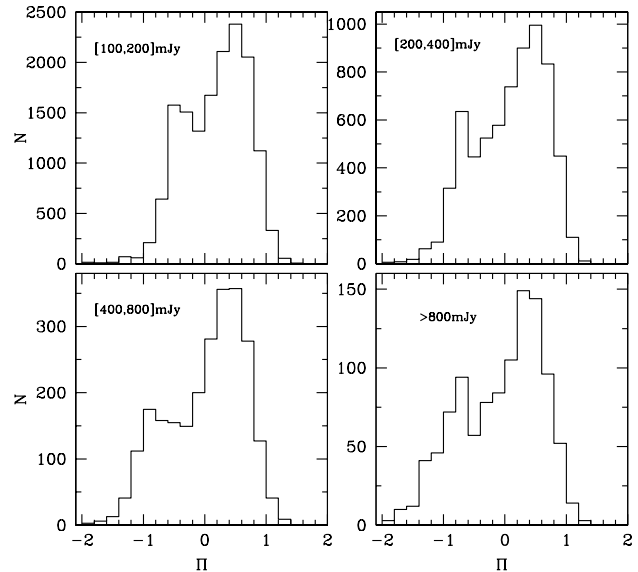
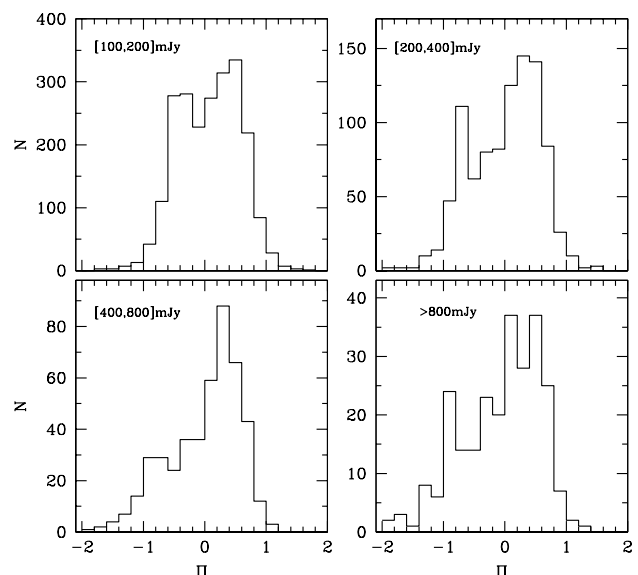

Figure 2. Polarization degree distribution of steep-spectrum NVSS sources for the flux density intervals specified in each panel.

Figure 3. As in Figure 2 but for flat-spectrum sources.

Table 2. Results of the χ^2 test for Π distributions at different fluxes. The distributions are binned in intervals of the 1% width. Probability values above the diagonal refer to flat-spectrum sources, those below the diagonal, to steep-spectrum sources.

(mJy)	100–200	200–400	400–800	> 800
100–200	–	0.28	0.91	0.95
200–400	2.1×10^{-4}	–	0.12	0.06
400–800	1.8×10^{-4}	4.8×10^{-2}	–	0.52
> 800	1.4×10^{-6}	6.1×10^{-3}	0.16	–

tween the polarization degree and the flux density for steep-spectrum sources: the median value of Π steadily decreases from 1.8% at 100–200 mJy to 1.1% at $S \geq 800$ mJy (we consider the median because it is less affected than the mean by instrumental polarization). A similar trend is not found for flat-spectrum sources, whose median values show only small fluctuations, all compatible with a constant value at the 1- σ level. Pearson's linear correlation coefficient r between the flux density and the polarization degree of sources is low for both flat (-0.017) and steep-spectrum (-0.034) sources, yielding a 30% probability of the null hypothesis (i.e., no correlation) in the flat case. However, the χ^2 test clearly rules out the possibility that the polarization degree distributions of steep-spectrum sources in the range 100–200 mJy and at higher flux density are drawn from the same parent distribution (probabilities of the order or less than 10^{-4} ; see Table 2). On the contrary, in the case of flat-spectrum sources, the test indicates consistency with the same parent distribution for all flux density ranges (in particular, a probability of 95% is found comparing the intervals at 100–200 mJy and > 800 mJy).

Differences in the Π distributions for flat-spectrum sources can be perceived in Figure 3 for $\Pi < 1\%$. However, they are probably not intrinsic but induced by instrumental effects: at low fluxes (100–400 mJy) only few sources are detected with $\Pi \lesssim 0.1\%$ because the noise rms contribution is $\simeq 0.3\%$; viceversa, at $S > 400$ mJy, where the noise is practically negligible, a significant tail of very low values of Π is observed. Finally, we note that artificial peaks in the distributions at $\Pi \simeq 0.1\text{--}0.25\%$ are produced by the residual instrumental polarization.

The origin of the anti-correlation in steep-spectrum sources is not clear yet. A possible explanation is a systematic increase of the mean redshift of sources with decreasing the flux density, which would entail a decrease of the Faraday rotation measure $\propto (1+z)^{-2}$. A moderate anti-correlation between mean redshift and flux density is indeed expected based on the T98 model. On the other hand, currently available data do not provide any evidence of a positive correlation between polarization degree and redshift of sources.

Contrary to M02, we do not find any evidence that the polarization of flat-spectrum sources depends on the flux density. The discrepancy is probably a consequence of the different separation in steep- and flat-spectrum sources. In M02, the fraction of NVSS flat-spectrum sources is very high ($\sim 44\%$), and roughly constant at every flux-density interval. It is possible that, not having taken into account the effect of the different angular resolution in the comparison between NVSS and GB6 flux densities, M02 have underes-

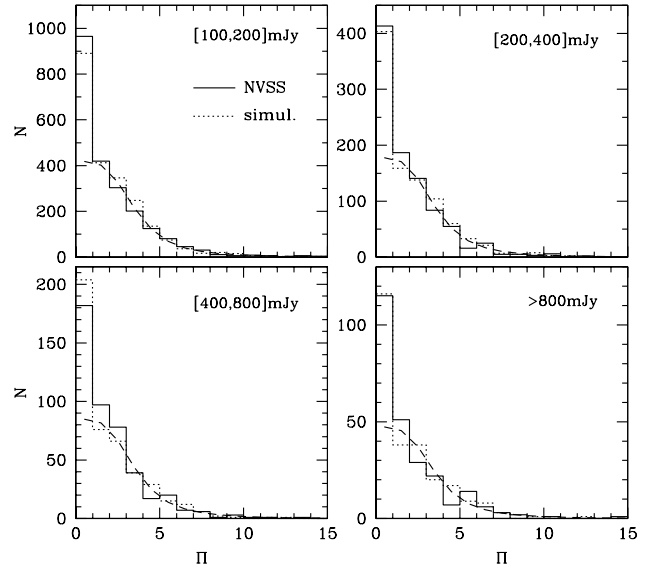


Figure 4. The Π distribution for NVSS flat-spectrum sources (solid histogram) compared with results of the simulated catalogue (dotted histogram). The dashed curves are the fit given by the first term of Eq. (2).

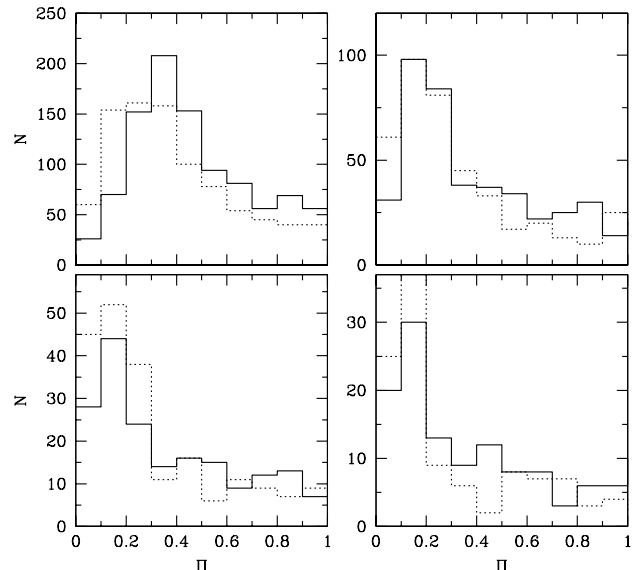


Figure 5. The same as in Figure 4 but for $\Pi = [0, 1]\%$.

timated the spectral index of a significant fraction of steep-spectrum sources, misclassifying them as flat-spectrum.

2.1 The 1.4 GHz Π probability distribution for flat-spectrum sources

The Stokes parameters Q and U , measured by the NVSS, are the sum of three terms:

Table 3. Polarimetric data on extragalactic radio sources.

Reference	ν (GHz)	N. sources	Comments
Eichendorf & Reinhardt (1979)	[0.4, 15]	510	multi-frequency data
Tabara & Inoue (1980)	[0.4, 10.7]	1510	multi-frequency data
Simard-Normandin et al. (1981)	[1.6, 10.5]	555	multi-frequency data
Perley (1982)	1.5, 4.9	404	
Rudnick et al. (1985)	[1.4, 90]	20	flat; multi-frequency data
Aller et al. (1992)	4.8, 14.5	62	35 flat, 27 steep; complete sample ($S_{5\text{GHz}} > 1.3 \text{ Jy}$)
Okudaira et al. (1993)	10	99	flat; complete sample ($S_{5\text{GHz}} > 0.8 \text{ Jy}$)
Nartallo et al. (1998)	273	26	flat
Condon et al. (1998)	1.4	$\sim 2 \times 10^6$	complete sample ($S_{1.4\text{GHz}} > 2.5 \text{ mJy}$)
Aller et al. (1999)	4.8, 14.5	41	BL LAC
Zukowski et al. (1999)	4.75	154	28 flat, 122 steep
Lister (2001)	43	30	flat; 90% complete sample ($S_{5\text{GHz}} > 1.3 \text{ Jy}$)
VLA Calibrators	5, 8.5, 22, 43	62	55 flat, 7 steep

$$Q, U(\text{obs}) = Q, U(\text{int}) + Q, U(\text{noise}) + Q, U(\text{res}), \quad (1)$$

where $Q, U(\text{int})$ are the intrinsic values, while the other two terms represent the contribution of the noise and of the residual instrumental polarization. We find that the distribution of $Q, U(\text{obs})$ for flat-spectrum sources can be reproduced adopting the following expression for the intrinsic distribution of polarization degrees at 1.4 GHz $\Pi_{1.4}$ (considering the flux density from the NVSS catalogue and a random distribution of polarization angles):

$$\mathcal{P}(\Pi_{1.4}) = \frac{a}{2.7 + 0.025\Pi_{1.4}^{3.7}} + bf(\Pi_{1.4}), \quad (2)$$

with

$$f(\Pi_{1.4}) = \begin{cases} \frac{1}{0.1} & \text{if } \Pi_{1.4} \leq 0.1 \\ 0 & \text{if } \Pi_{1.4} > 0.1 \end{cases}$$

The values of the coefficients ($a = 0.51$, $b = 0.24$) are determined by the condition that the observed fraction of sources with $\Pi_{1.4} < 1\%$ has to be reproduced. The first term in Eq. (2) is the best fit for the $\Pi_{1.4}$ distribution of sources with $100 \leq S < 200 \text{ mJy}$ and $\Pi_{1.4} \geq 1\%$ (it is shown by the dashed lines in Figure 4). The second term corresponds to a population of nearly unpolarized sources. In fact, for about 20% of the sources, the polarization degree given by the NVSS catalogue is less than 0.4%; these values are only upper limits to the intrinsic polarization since they can be accounted for by instrumental polarization and noise. For such sources we have assumed an intrinsic polarization uniformly distributed between 0 and 0.1%.

The distributions of the noise and of the residual instrumental polarization for Q and U are assumed to be Gaussian with zero mean and variance 0.29 mJy and $0.001S$, respectively.

Figures 4 and 5 compare the polarization degree distributions of NVSS sources with the results of our simulations. The good agreement at every flux-density interval is evident and it is confirmed by the Kolmogoroff-Smirnov (K-S) test. The probability that the two sets of data come from the same distribution is: 6×10^{-3} , 0.23, 0.30, 0.60 for $100-200 \text{ mJy}$, $200-400 \text{ mJy}$, $400-800 \text{ mJy}$, $> 800 \text{ mJy}$ respectively. The fit is not satisfactory only for the low polarization portion ($\Pi \lesssim 0.5\%$) of the distribution for the $100-200 \text{ mJy}$ interval (see Figure 5), probably due to our difficulty in correctly modelling the instrumental polarization.

3 POLARIZATION DATA FOR EXTRA-GALACTIC RADIO SOURCES AT $\nu > 1.4 \text{ GHz}$

Data on the polarization of extragalactic radio sources at frequencies higher than 1.4 GHz are rather limited, particularly above 5 GHz. At high frequencies, where Faraday depolarization should be negligible, data are restricted to incomplete samples of few tens of objects (see Table 3).

Complete samples are essential to avoid selection biases. For this reason we have extracted from the MIT-Green Bank surveys (Bennett et al. 1986, Langston et al. 1990, Griffith et al. 1990, Griffith et al. 1991) a complete sub-sample of sources with $S_{5\text{GHz}} > 1.4 \text{ Jy}$ in the following sky areas:

$$|b| > 10^\circ, \quad -0^\circ.5 < \delta < 19^\circ.5$$

$$5^\circ \leq \text{ra} < 19^\circ, \quad 20^\circ < \text{ra} < 4^\circ, \quad 17^\circ < \delta < 39^\circ.15$$

$$15^\circ.5 < \text{ra} < 19^\circ, \quad 20^\circ < \text{ra} < 2^\circ.5, \quad 37^\circ < \delta < 51^\circ,$$

and we complemented it with sources from the Pearson-Readhead survey (Pearson & Readhead 1981, 1988) at $\delta > 35^\circ$ and $|b| > 10^\circ$. Polarization measurements at 4.8 GHz were found for 139 ($\sim 95\%$) of sources in the final sample (hereafter MG+ sample). Each source was then identified in the NVSS and the spectral index between 1.4 and 4.8 GHz was estimated.

Table 4 compares the values of the mean polarization degree from samples at different frequencies, while Figures 6-7 show the polarization degree distributions for flat- and steep-spectrum sources. For flat-spectrum sources, $\langle \Pi \rangle$ increases steadily between 1.4 and 14.5 GHz, although by only a factor 1.5, and keeps constant between 15 and 43 GHz in the samples of Aller et al. (1992) and of Lister (2001) (note that these flat-spectrum samples are identical, except for three sources present at 15 GHz but not at 43 GHz). A steady, but weak, increase of the polarization degree with the frequency is also found in the case of VLA calibrators¹, simultaneously observed at 5 frequencies between 5 and 43 GHz. In general, data on flat-spectrum sources indicate that this population is not strongly affected by Faraday depolarization and that the polarization degree might

¹ <http://www.aoc.nrao.edu/~smyers/calibration/>

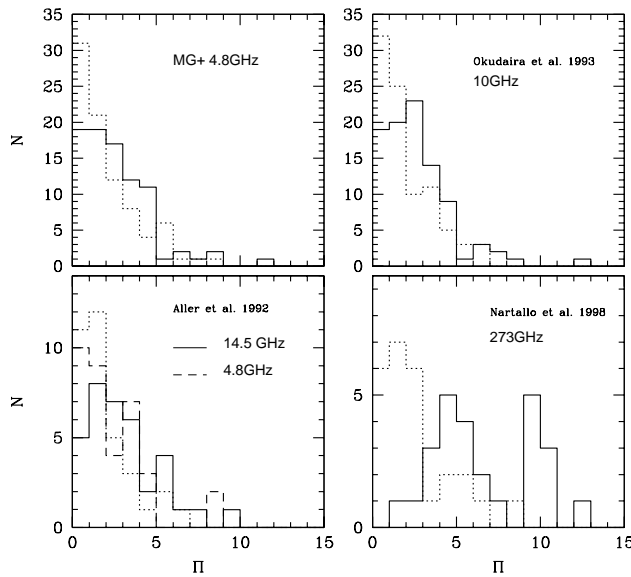


Figure 6. Π distribution of flat-spectrum sources for different samples at $\nu > 1.4$ GHz (solid histograms). Dotted histograms show, for comparison, the Π distributions of the same sources at 1.4 GHz, based on NVSS measurements.

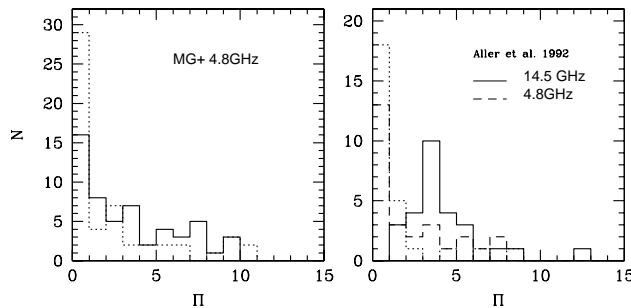


Figure 7. Same as in Figure 6 but for steep-spectrum sources.

become frequency independent already at $\nu \gtrsim 15$ GHz. On the other hand, a significantly higher mean polarization degree, $\langle \Pi \rangle = 6.6\%$, corresponding to an increase by nearly a factor of 3 from the value at 1.4 GHz, has been found by Nartallo et al. (1998) for a sample of blazars at mm/sub-mm wavelengths, where we are probably observing regions very close to the active nucleus, whose emission is self-absorbed at lower frequencies. Thus, apart from the fact that conclusions based on incomplete samples need always to be taken with care, a large increase of the polarization degree from 1.4 GHz to 300 GHz can be a consequence of the higher uniformity of the magnetic field in the innermost regions.

Data on steep-spectrum sources are limited to $\nu \lesssim 15$ GHz (see Table 3), and show a clear increase of the polarization degree with frequency. For the Aller et al. (1992) sample $\langle \Pi \rangle = 1.3\%, \simeq 2.3\%, \simeq 4.1\%$ at $\nu = 1.4, 4.8, 14.5$ GHz respectively, while for the MG+ sample $\langle \Pi \rangle$ changes from 2.4% at 1.4 GHz to 3.3% at 4.8 GHz. The factor of 3 increase between 1.4 and 14.5 GHz is comparable to the result of M02 from a sample of ~ 130 objects, and

Table 4. Average polarization degree at various frequencies for different samples.

		N	ν (GHz)	$\langle \Pi \rangle$	σ
MG+	flat	85	1.4	2.0	1.9
			4.8	2.6	2.1
	steep	54	1.4	2.4	3.1
			4.8	3.3	2.9
Okudaira et al. (1993)	flat	89	1.4	1.8	1.7
			10	2.7	2.1
Aller et al. (1992)	flat	35	1.4	1.8	1.7
			4.8	2.3	2.0
			14.5	3.0	2.2
	steep	27	1.4	1.3	2.1
			4.8	2.3	2.4
			14.5	4.1	2.2
	flat	32	1.4	2.0	1.8
			43	3.0	2.2
Nartallo et al. (1998)	flat	26	1.4	2.4	2.0
			273	6.6	3.0
VLA Calibrators	flat	55	1.4	1.9	2.1
			48	5	2.1
			45	8.5	2.3
			47	22	2.4
			53	43	2.4

Data at 1.4 GHz come from the NVSS.

is compatible with a strong Faraday depolarization at few-GHz frequencies.

4 THE Π DISTRIBUTION OF FLAT-SPECTRUM SOURCES AT HIGH FREQUENCIES

As discussed in Sect. 2, the NVSS data are consistent with the polarization degree of flat-spectrum sources being essentially independent of flux density. If so, the polarization properties of bright sources ($S \gtrsim 1$ Jy), for which high frequency data are available, can be assumed to hold also for much fainter sources.

First of all, we check whether the polarization of a source at 1.4 GHz is correlated to its value at higher frequencies. Indeed, the previously mentioned, frequency dependent effects (Faraday depolarization and the fact that at different frequencies we may effectively observe different emitting regions) could spoil such correlation. If so, low-frequency data would not be representative of high frequency polarization properties. The Pearson's linear correlation coefficient r between the polarization at 1.4 and 4.8 GHz of the sources in the MG+ and Aller et al. (1992) samples is ~ 0.6 corresponding to a probability of the null hypothesis, i.e. no-correlation, of $\lesssim 10^{-6}$. The correlation is less clear in the samples at higher frequencies ($r \sim 0.2$ and null-hypothesis probability of $\gtrsim 10^{-2}$). However, these results are probably affected by the variability of sources, because we are comparing data taken at different epochs. On the contrary, a strong correlation ($r > 0.5$ and null-hypothesis probability $< 10^{-4}$) between 5 and 43 GHz is found for the VLA cal-

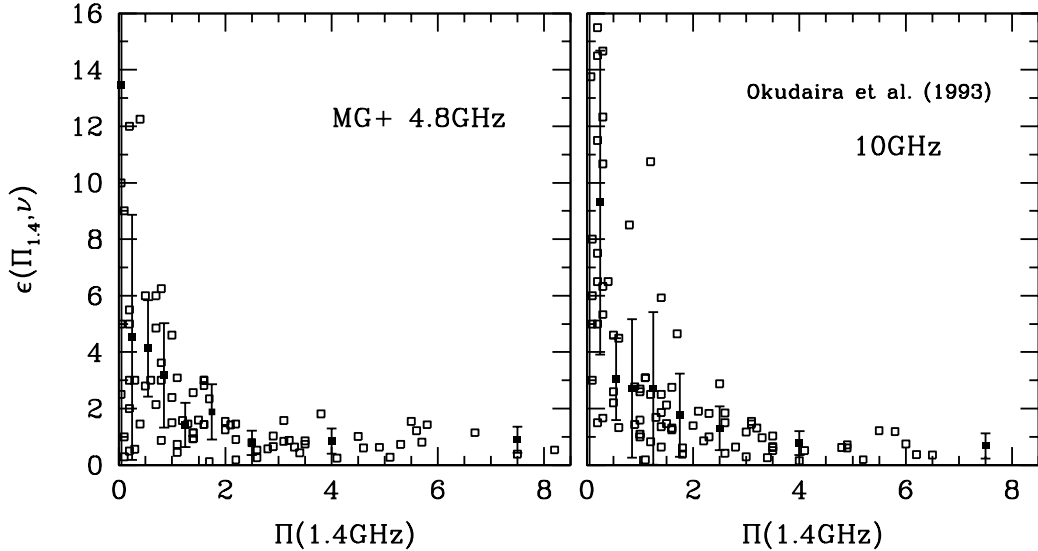


Figure 8. Values of ϵ as a function of Π at 1.4 GHz for MG+ sources (left plot) and for the Okudaira et al. (1993) sample at 10 GHz (right plot). Points with the error bar give $\langle \epsilon \rangle$ with its dispersion.

ibrators, whose polarization is measured simultaneously at all frequencies.

Consequently, the polarization degree of a source at frequency ν can be written in term of its value at 1.4 GHz ($\Pi_{1.4}$) as

$$\Pi(\nu) = \Pi_{1.4}\epsilon(\Pi_{1.4}, \nu), \quad (3)$$

where the factor ϵ is the increase of the polarization degree from the value at 1.4 GHz. We find that ϵ itself is a function of the polarization degree at 1.4 GHz: Fig. 8 shows ϵ as function of $\Pi_{1.4}$ for the sources in the MG+ and Okudaira et al. (1993) samples, while Table 5 gives the average ϵ and its dispersion for different bins of $\Pi_{1.4}$. For sources with $\Pi_{1.4}$ above a few percent, $\langle \epsilon \rangle$ is close to unity at all frequencies, but it can take very large values (up to more than 10) if $\Pi_{1.4}$ is very small.

We can conclude that: (i) the typical intrinsic polarization degree of flat-spectrum sources is of 2–5%; (ii) high values of the polarization degree are unlikely (sources with $\Pi \gtrsim 10\%$ are rare in the whole range of frequencies analysed), probably due to the low degree of the uniformity of magnetic fields in radio sources; (iii) Faraday depolarization is probably the cause of the large number of sources observed with very low polarization degree (in fact, flat-spectrum sources with extreme values of RM have been observed by Stanghellini et al. 1998, Taylor 2000 and Pentericci et al. 2000). Finally, as already pointed out for $\langle \Pi \rangle$, the behaviour of $\epsilon(14.5\text{GHz})$ and $\epsilon(43\text{GHz})$ is very similar, confirming that the polarization is weakly frequency dependent for $\nu > 15\text{GHz}$. On the other hand, $\langle \epsilon \rangle$ at mm wavelengths is higher than at GHz frequencies in all $\Pi_{1.4}$ bins.

Using MG+ and Okudaira et al. (1993) data, we get a simple analytical formula for the mean value of $\epsilon(\Pi_{1.4}, \nu)$:

$$\langle \epsilon(\Pi_{1.4}, \nu) \rangle = A(\nu) \exp(-3.2\Pi_{1.4}^{0.35}) + 0.8, \quad (4)$$

where the frequency dependence appears only in the coefficient $A(\nu)$ which takes the values 38, 50 and 108 at $\nu = 4.8$,

10 and 273 GHz respectively. Using these three values, we obtain a law, $A(\nu) = 72 \ln(0.75\nu^{0.3} + 0.5)$, which allows us to compute $\langle \epsilon(\Pi_{1.4}, \nu) \rangle$ at every frequency. The large dispersions around the mean values of ϵ are described by a fit similar to Eq. (4), obtained interpolating the values of the variance of ϵ in the $\Pi_{1.4}$ bins:

$$\sigma_{\langle \epsilon \rangle}(\Pi_{1.4}, \nu) = B(\nu) \exp(-5\Pi_{1.4}^{0.3}) + 0.5. \quad (5)$$

The factor B is equal to 100 or 210 at $\nu = 4.8$ or 10 GHz, respectively, and it remains constant at higher frequencies (we use a linear interpolation at $\nu \leq 10\text{GHz}$).

The above expressions for $\langle \epsilon(\Pi_{1.4}, \nu) \rangle$ and for its variance are used to estimate the polarization degree distributions of flat-spectrum sources at every frequency in the range [5, 300] GHz, starting from that of $\Pi_{1.4}$: the increase factor ϵ is modelled by a Gaussian distribution which is cut at negative ϵ and whose mean value and variance are given by Eq. (4) and (5). In Figure 9 we give examples of the Π probability distributions between 1.4 and 100 GHz, using a simulated sample of 1000 sources [the probability distribution at 1.4 GHz is obtained from Eq. (2)]. The Figure shows also the observed distributions at $\nu \leq 15\text{GHz}$, scaled to the total number of simulated sources; the good agreement between data and simulations is apparent. Moreover, the K-S test finds high probabilities ($\gtrsim 0.3$) that the observed distributions are realizations of the probability distributions resulting from our simulations. A significant agreement is also found with the recent data at 18 GHz by Ricci et al. (2003).

Finally, exploiting the T98 model, we generate simulations of the polarized intensity of the sky at 30 and 100 GHz including radio sources and the CMB (see Figure 10). We can directly compare the importance of the contribution of radio sources at the two frequencies: at 30 GHz a lot of sources are evident in the map, superposed to the CMB signal, while at 100 GHz their presence is far less conspicuous.

Table 5. Average values of ϵ and of its variance as a function of $\Pi_{1.4}$.

	$\Pi_{1.4}$	N	$\langle \epsilon \rangle$	σ
MG+ (4.8 GHz)	[0,0.1)	9	13.5	13.7
	[0.1,0.4)	10	4.52	4.33
	[0.4,0.7)	6	4.13	1.70
	[0.7,1)	7	3.18	1.84
	[1,1.5)	11	1.42	0.79
	[1.5,2)	9	1.88	0.98
	[2,3)	10	0.78	0.43
	[3,5)	12	0.86	0.45
	> 5	9	0.90	0.46
Okudaira et al. (1993) (10 GHz)	[0,0.1)	9	27.3	31.0
	[0.1,0.4)	15	9.30	5.38
	[0.4,0.7)	5	3.05	1.45
	[0.7,1)	8	2.72	2.45
	[1,1.5)	14	2.72	2.70
	[1.5,2)	7	1.77	1.48
	[2,3)	11	1.30	0.77
	[3,5)	14	0.78	0.42
	> 5	6	0.68	0.45
Aller et al. (1992) (4.8 GHz)	[0,0.1)	1	1.14	—
	[0.1,1)	10	3.90	3.28
	[1,2)	12	1.77	1.10
	[2,4)	8	0.67	0.39
	> 4	4	1.08	0.47
(14.5 GHz)	[0,0.1)	1	44.6	—
	[0.1,1)	10	8.94	9.38
	[1,2)	12	1.98	0.84
	[2,4)	8	1.46	1.37
	> 4	4	0.70	0.56
Lister (2001) (43 GHz)	[0,0.1)	0	—	—
	[0.1,1)	9	7.43	4.54
	[1,2)	11	2.07	1.27
	[2,4)	8	1.33	0.93
	> 4	4	0.56	0.41
Nartallo et al. (1998) (273 GHz)	[0,0.1)	2	41.5	27.5
	[0.1,1)	6	8.10	3.48
	[1,2)	6	4.96	1.95
	[2,4)	6	3.05	1.28
	> 4	6	1.10	0.38

5 ESTIMATE OF POLARIZATION POWER SPECTRA

Using the statistical characterization of the polarization degree described in the previous section, we are able to estimate the angular power spectrum (APS) of polarization fluctuations due to extragalactic radio sources. We adopt the T98 model in order to predict the source number counts at cm and mm wavelengths (the model number counts are scaled by a factor 0.75 to be in agreement with the WMAP data).

We assume the spatial distribution of sources to be Poissonian. The contribution of radio-source clustering to the power spectrum is, in fact, small and can be neglected if sources are not subtracted down to very low flux limits (the clustering is noticeable only at relatively small fluxes, $S \leq 100$ mJy; see T98 and Toffolatti et al. 2003). Then the

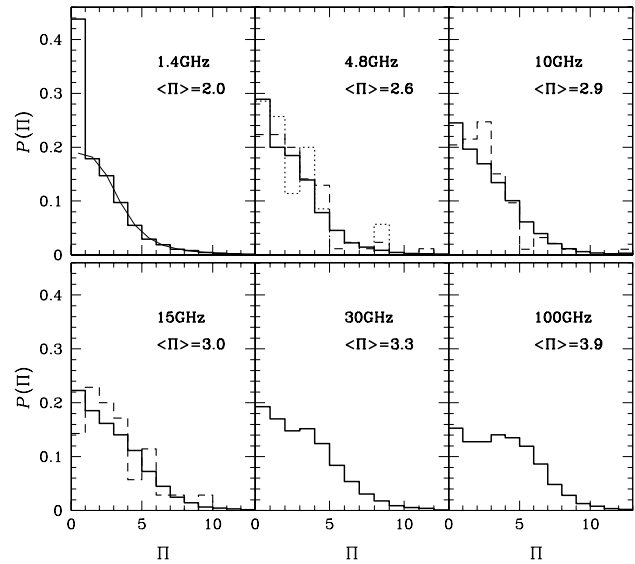


Figure 9. Simulated Π distributions at several frequencies between 1.4 and 100 GHz. The mean value of Π is also indicated. The solid line in the plot at 1.4 GHz represents the first term of Eq. (2). We report also the observed Π distributions, scaled to the number of simulated sources: 4.8 GHz data refer to the MG+ (dashed histogram) and the Aller et al. (1992) (dotted histogram) samples; 10 GHz and at 15 GHz data to the Okudaira et al. (1993) and Aller et al. (1992) samples respectively.

power spectrum is independent of the angular scale, and can be computed in the limit of small scales. Under these conditions, we have $C_{E\ell} + C_{B\ell} = C_{Q\ell} + C_{U\ell}$ (Tucci et al. 2002). Moreover, because point sources contribute, on average, equally to the E -, B -mode and to Q , U power spectra (Seljak 1997, M02), $C_{E\ell} \simeq C_{B\ell} \simeq C_{Q\ell} \simeq C_{U\ell}$ (in the following we refer to any of these spectra as the polarization APS).

We estimate the point-source polarization APS in two ways: first as the product of the temperature power spectrum, $C_{I\ell}$, and the mean squared polarized intensity; second, directly from the number counts of Q (or U). In both cases, we exploit the Π probability distributions obtained in the previous section.

Tegmark & Efstathiou (1996) have shown that the APS of intensity fluctuations produced by Poisson-distributed sources can be written as:

$$C_{I\ell} = N \langle S^2 \rangle = \int_0^{S_c} n(S) S^2 dS, \quad (6)$$

where N and $n(S)$ are, respectively, the total and the differential number of sources per steradian, and S_c is the minimum flux density of sources that can be individually detected and removed.

In analogy to Eq. (6), the Q APS will be

$$C_{Q\ell} = N \langle Q^2 \rangle. \quad (7)$$

The Stokes parameter Q can be written in terms of the polarization degree $p = \Pi/100$ and of the polarization angle in the chosen reference system, ϕ , as $Q = Sp \cos(2\phi)$. Because

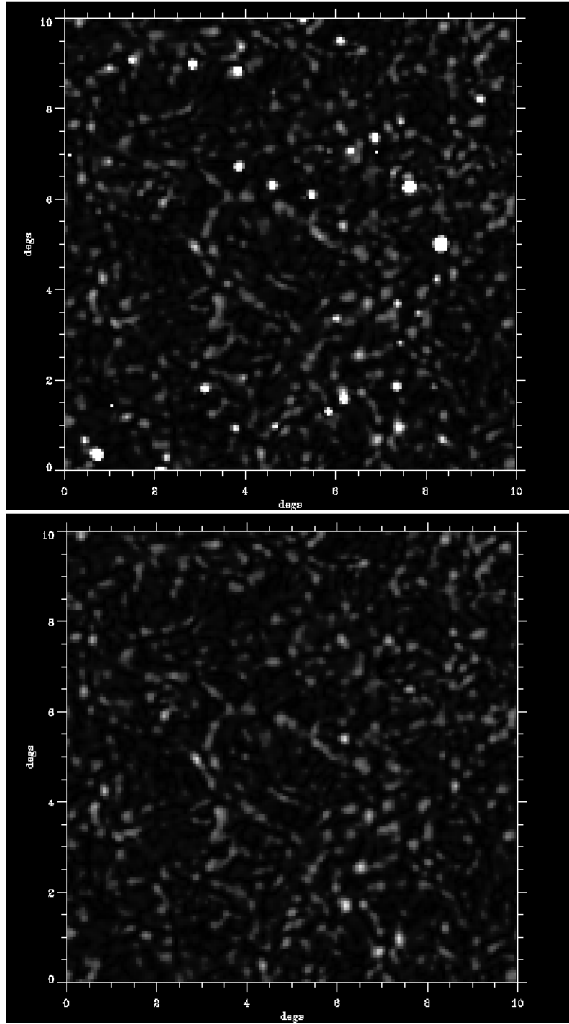


Figure 10. Simulated polarized skies at 30 (upper plot) and 100 GHz (lower plot) generated including extragalactic radio sources and CMB radiation (standard CDM model). The sources are far less conspicuous at 100 GHz than at 30 GHz.

we find S , p and ϕ to be independent variables in the NVSS survey (at least in the case of flat-spectrum sources), we obtain

$$\begin{aligned} C_{Q\ell} = N < Q^2 > &= N < S^2 p^2 \cos^2(2\phi) > \\ &= N < S^2 > < p^2 > < \cos^2(2\phi) > \\ &= 1/2 C_{I\ell} < p^2 >, \end{aligned} \quad (8)$$

where the factor 1/2 arises because of the uniform distribution of polarization angles.

At a frequency ν , the mean squared value of the polarization degree, $< p_\nu^2 >$, is:

$$< p_\nu^2 > = 10^{-4} \int_0^{100} \mathcal{P}(\Pi_\nu) \Pi_\nu^2 d\Pi_\nu, \quad (9)$$

where the probability distribution of Π_ν at frequency ν , $\mathcal{P}(\Pi_\nu)$, is related to $\mathcal{P}(\Pi_{1.4})$ [given in Eq. (2)]:

$$\begin{aligned} \mathcal{P}(\Pi_\nu) &= \mathcal{P}(\Pi_{1.4}) \frac{d\Pi_{1.4}}{d\Pi_\nu} \\ &= \frac{\mathcal{P}(\Pi_{1.4})}{|\epsilon_\nu(\Pi_{1.4}) - 1.12[\epsilon_\nu(\Pi_{1.4}) - 0.8]\Pi_{1.4}^{0.35}|}. \end{aligned} \quad (10)$$

Here we have used the relation $\Pi_\nu = \Pi_{1.4}\epsilon_\nu(\Pi_{1.4})$ and Eq. (4) for the mean value of ϵ_ν . For example, we find $< p^2 >^{1/2} = 0.041$ at 30 GHz and $< p^2 >^{1/2} = 0.046$ at 100 GHz.

Finally, it is easy to demonstrate that the cross-correlation TQ spectrum is

$$C_{TQ\ell} = < S^2 p \cos(2\phi) > = 0. \quad (11)$$

The previous method assumes that sources are removed from polarization maps using total intensity data. However, not all the experiments observing the sky polarization are able to measure the total intensity [see, for example, the experiments: SPOrt (Carretti et al. 2003); COMPASS (Farese et al. 2003); CAPMAP (Barkats 2003)]. In this case, sources have to be detected and removed directly from Q and U maps. Therefore, we need to compute the Q APS using the differential sources counts $n(Q)$, as in Eq. (6):

$$C_{Q\ell} = \int_{-Q_c}^{Q_c} n(Q) Q^2 dQ, \quad (12)$$

where Q_c is the lowest value of Q of sources that can be individually detected and removed from polarization maps. The counts $n(Q)$ can be obtained from the probability distribution of the three Stokes parameters that describe the linear polarization, $\mathcal{P}(S, Q, U)$, as

$$n(Q) = \int_{-U_c}^{U_c} dU \int_0^\infty \mathcal{P}(S, Q, U) dS. \quad (13)$$

The probability $\mathcal{P}(S, Q, U)$ is related to the probability distribution of S , of the polarization degree $p = \sqrt{Q^2 + U^2}/S$ and of the polarization angle $\phi = 1/2 \arctan(U/Q)$, through

$$\mathcal{P}(S, Q, U) = \mathcal{P}(S, p, \phi) \det \mathcal{J} \begin{pmatrix} S & p & \phi \\ S & Q & U \end{pmatrix}, \quad (14)$$

where \mathcal{J} is the Jacobian matrix of the transformation $(S, Q, U) \rightarrow (S, p, \phi)$:

$$\det \mathcal{J} \begin{pmatrix} S & p & \phi \\ S & Q & U \end{pmatrix} = \frac{1}{2S\sqrt{Q^2 + U^2}}. \quad (15)$$

As previously noted, the variables S , p and ϕ are independent, and therefore

$$\mathcal{P}(S, p, \phi) = \mathcal{P}(S)\mathcal{P}(p)\mathcal{P}(\phi) = N^{-1}n(S)\mathcal{P}(p)/\pi; \quad (16)$$

$n(S)$ is provided by the T98 model and $\mathcal{P}(p) = 100\mathcal{P}(\Pi)$ by Eq. (10). Finally:

$$\begin{aligned} n(Q) &= \frac{1}{\pi} \int_0^{U_c} \frac{dU}{\sqrt{Q^2 + U^2}} \times \\ &\times \int_0^\infty \frac{n(S)\mathcal{P}(\sqrt{Q^2 + U^2}/S)}{S} dS. \end{aligned} \quad (17)$$

Figure 11 shows our estimates of the polarization APS using the two methods discussed above, at the frequencies 30, 44, 70 and 100 GHz. In each panel, the two dotted curves are computed using Eq. (8) (i.e., the first method), and $S_c = 1 \text{ Jy}$ (upper line) or the frequency dependent detection limit (see caption) obtained by Vielva et al. (2003) for the Planck mission using the spherical Mexican hat wavelet to remove bright sources (lower line). The latter limit, multiplied by $\sqrt{2}$, is used for Q_c (and U_c) in Eq. (12) (assuming

that the source removal algorithm has a similar efficiency for polarization maps as for intensity ones). The factor $\sqrt{2}$ arises if the noise in temperature and polarization are related by $\sigma_T^2 = \sigma_P^2/2$. The extrapolation of the polarization degree distribution at 1.4 GHz to frequencies between 30 and 100 GHz is obtained using Eq. (3) and the mean value of ϵ , Eq. (4). The uncertainty on the polarization APS due to the high-frequency extrapolation can be estimated by different realizations of Π distributions generated following the recipe we describe in section 4. We find that the variance is small, a few percent of the average spectrum (the number of sources is large enough to assure the sample variance to be negligible).

As discussed in section 4, if the data of Nartallo et al. (1998) are disregarded, the polarization degree appears to be weakly dependent on the frequency for $\nu > 15$ GHz. Assuming the Π distribution to be constant above 15 GHz, the amplitude of the polarization APS decreases weakly with respect to previous estimates: $\sim 10\%$ at 30 GHz and $\sim 30\%$ at 100 GHz (the differences are visibly appreciable only in the 100 GHz panel of Fig. 11). These latter estimates can be considered as lower limits and, together with the ones using the high-frequency extrapolation, provide us with two boundaries within which we expect to find the real polarization APS.

We have verified that the results from the two methods agree when the bright source removal is equivalent. Otherwise, as illustrated by Fig. 11, estimates based on Eq. (8) are significantly lower than those using Eq. (12): the difference is nearly a factor 10 if we take $Q_c = U_c = \sqrt{2}S_c$ (in the real case, however, we expect that $Q_c = U_c > \sqrt{2}S_c$, further increasing the difference). This is easily understood: adopting the limit on total flux density we are subtracting many more sources than we can do using only polarization maps.

The previous estimates are obtained assuming that the polarization degree distribution for steep-spectrum sources is the same as for the flat-spectrum ones, although the results reported in Table 4 and by M02 indicate that steep-spectrum sources are, on average, more polarized, at least at low frequencies. However, the contribution of steep-spectrum sources to the polarization APS is anyway very small at $\nu > 40$ GHz.

The likely correction to our results at 30 GHz can be estimated as follows. The VSA survey at 15 GHz (Waldrum et al. 2003) finds a 25 percent of steep-spectrum sources for $S_{15} \geq 100$ mJy and a 44 percent for $S_{15} \geq 25$ mJy, corresponding to a contribution to $C_{I\ell}$ of 30% if $S_c = 1$ Jy and of 43% if $S_c = 200$ mJy (we assume that the fraction of steep-spectrum sources increases to 75% if $S_{15} < 25$ mJy). Their contribution to the APS is reduced by a factor 3 at 30 GHz if their average spectral index is -0.8 between 15 and 30 GHz (a rather conservative assumption since the high frequency spectra steepen due to electron ageing effects). From the NVSS catalogue we find that $\langle \Pi_{1.4}^2 \rangle^{1/2} \simeq 2.6\%$ for steep-spectrum sources with $S_{1.4} \geq 200$ mJy. Now, assuming that the polarization degree increases, on average, by a factor of 3 from 1.4 GHz to high frequencies, we obtain that our estimates of the polarization APS by Eq. (8) must be multiplied at 30 GHz by 1.3 or 1.4 in the case that $S_c = 1$ Jy or 200 mJy respectively (dot-dashed lines in the 30 GHz plot of Figure 11).

6 DISCUSSIONS AND CONCLUSIONS

The main goal of the present paper is to provide estimates of the contamination of CMB polarization maps by extragalactic radio sources. This task is particularly complicated because of the lack of polarimetric data at the frequencies where the CMB is observed.

The richest data on the polarization properties of radio sources comes from the NVSS survey, which provides a very large and complete catalogue of extragalactic sources at 1.4 GHz. Exploiting the spectral information obtained combining the NVSS with the GB6 survey at 4.8 GHz, we have analyzed the properties of steep- and flat-spectrum sources. The former population shows an anti-correlation of the polarization degree with the flux density, already pointed out by M02. On the contrary, for flat-spectrum sources the distributions of the polarization degree for different flux-density ranges do not show any significant variation and its mean value is constant and quite low, around 2%. For this class of sources we find a fit that accurately describes the polarization degree distribution for all sources with $S \geq 100$ mJy.

Exploiting the available data at $\nu > 1.4$ GHz, we have investigated how the polarization degree of sources varies with frequency. Data on steep-spectrum sources, available only up to 15 GHz, highlight a strong increase of the mean polarization degree with frequency, consistent with substantial Faraday rotation measures. On the other hand, the mean polarization degree of flat-spectrum sources shows only a weak increase between 1.4 and 15 GHz, and appears to remain essentially constant at higher frequencies. However, the high values of the polarization degree found at mm wavelengths by Nartallo et al. (1998) may be an indication that new, more polarized, components show up there.

For flat-spectrum sources, we have derived an analytic function allowing us to extrapolate to any frequency the distribution of polarization degrees at 1.4 GHz. We notice that only sources with $\Pi_{1.4} < 1\%$ increase significantly their polarization degree between 5 and 43 GHz. These sources may be the only ones with really strong Faraday depolarization at 1.4 GHz. In general, at $\nu \gtrsim 5$ GHz the polarization degree of flat-spectrum sources is typically of a few percent (it rarely exceeds 10%), and is weakly dependent on the frequency.

Using this analytic function, we estimate the power spectrum of polarization fluctuations induced by extragalactic radio sources, by means of the two methods described in Section 5. In particular, we consider for the first time the case whereby the removal of the brightest sources can be only done using polarization data. In this case, the source subtraction is far less efficient than if total flux data can be used and, as a consequence, the amplitude of the source power spectrum can be up to a factor of 10 higher. Total intensity data are, therefore, essential information in order to reduce the contamination of CMB polarization maps. In Figure 11 we show the estimated contribution of undetected radio sources to the polarization signal observed by the DASI experiment at 30 GHz: if indeed all the sources with the flux density higher than 50 mJy have been removed, the residual contamination is extremely small.

We have focused our analysis on flat-spectrum sources, since they are the dominant population at least up to 100 GHz. Steep-spectrum sources are taken into account only at 30 GHz, while they are disregarded at higher fre-

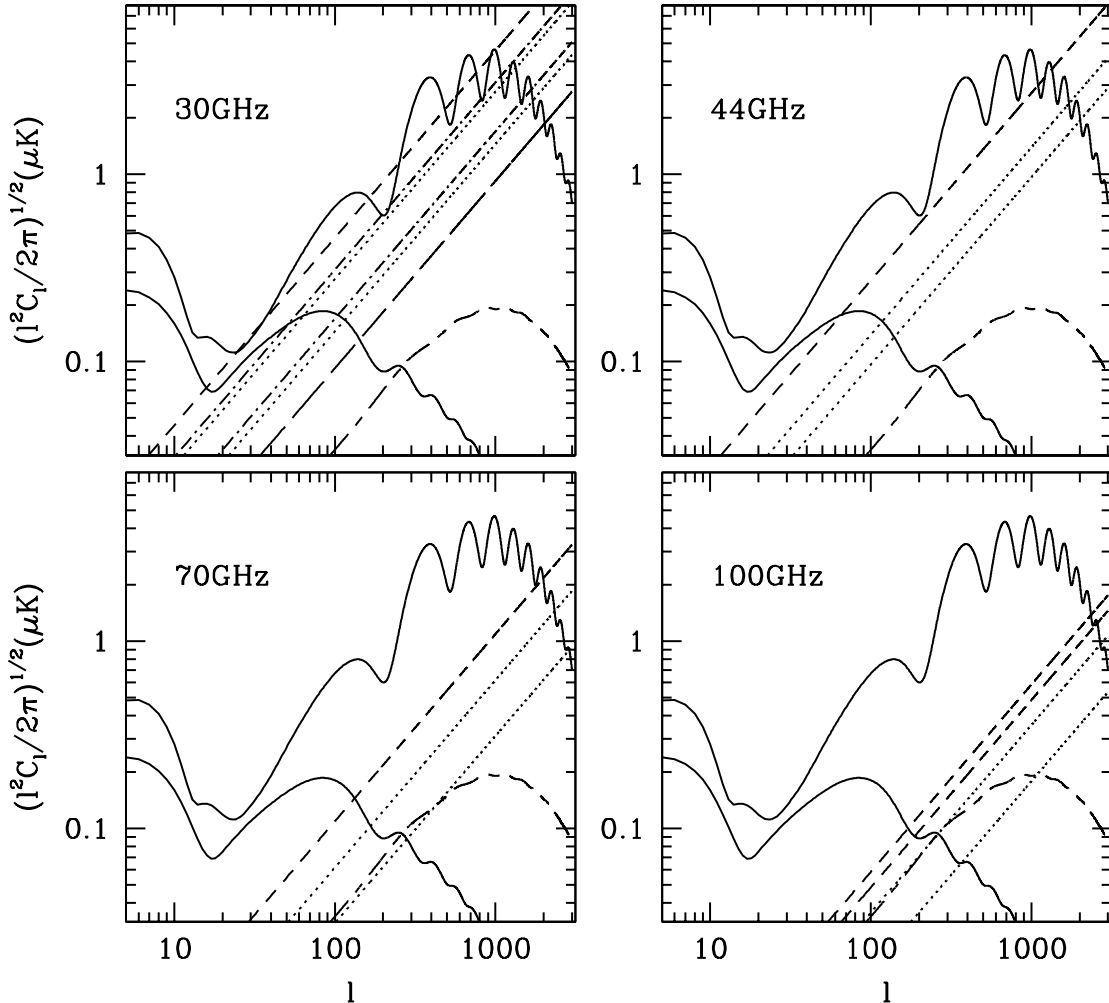


Figure 11. Polarization power spectrum produced by extragalactic radio sources compared to the E - and B -mode CMB spectrum (CDM model with $\Omega_\Lambda = 0.7$, re-ionization optical depth $\tau = 0.17$ and tensor-to-scalar ratio $r \simeq 0.5$). The short-long dashed lines are the B -mode component induced by gravitational lensing. The CMB and lensing spectra are computed with CMBFAST (Seljak & Zaldarriaga 1996). The APS for extragalactic radio sources are computed using the first method with $S_c = 1$ Jy (upper dotted lines) and S_c estimated by Vielva et al. (2003) for the Planck mission (200, 400, 250, 200 mJy at 30, 44, 70, 100 GHz; lower dotted lines), and using the second method with $Q_c = U_c = \sqrt{2}S_c$, where S_c is that from Vielva et al. (2003) (dashed lines). In the plot at 30 GHz, the dot-dashed lines corresponds to the estimates by the first method taking into account the correction for the contribution of steep-spectrum sources (see text); the long dashed line is our estimate for the contribution of undetected sources in the DASI experiment. In the plot at 100 GHz, the lower dashed line is the APS computed assuming the Π distribution to become frequency-independent for $\nu > 15$ GHz.

quencies. About the GPS sources, large uncertainties are still present on their abundance. The WMAP data at 33 GHz detected 16 sources with inverted spectra ($\alpha < -0.4$) over a total of 155 sources with $S > 1.2$ Jy. The multifrequency data summarized by Trushkin (2003) indicate that most of them are likely to be blazars (flat-spectrum quasars or BL Lacs) whose radio emission is dominated by a single emitting region (a knot in the jet) caught during a flare. Thus, the surface density of bright GPS sources peaking at high radio frequencies is likely to be several times lower than predicted by the De Zotti et al. (2000) models, even in the case of an intrinsic distribution of peak frequencies not extending above

~ 200 GHz. According to the latter model (which, in the light of WMAP sources, provides rather generous upper limits), at $\nu = 100$ GHz, the contribution of GPS sources to the total intensity APS is at the few percent level. Furthermore, the polarization degree of bona-fide GPS sources is very low at cm wavelengths. GPS galaxies generally have fractional polarization below 0.3% (many are undetected below 0.1% levels); GPS quasars have higher polarization than galaxies, but lower (at 6 cm) than non-GPS quasars (O'Dea et al. 1990; Stanghellini et al. 1998; Stanghellini 1999). Thus, the contribution of GPS sources to the polarization APS is likely to be even lower than to the total intensity APS.

It is interesting to compare our results on extragalactic radio sources with the E- and B-mode spectra of the CMB radiation (see Figure 11). First of all, we notice that the CMB E-mode APS increases with ℓ in a similar way to the point-source spectrum in the range $30 \lesssim \ell \lesssim 10^3$. At these angular scales, radio sources yield a relevant contribution to the E-mode polarization only for $\nu \lesssim 40$ GHz; in any case, also at these frequencies, they are not a serious problem for measurements of the CMB E-mode APS when the brightest sources are removed. At higher frequencies the cosmological signal is dominant at least up to $\ell \sim 2000$ or more.

On the other hand, extragalactic radio sources can be a critical factor for the detection of the CMB B-mode component: the cosmological $C_{B\ell}$ is characterized by a peak at $\ell \sim 100$ whose amplitude is directly related to the inflation model and, in particular, to the ratio between the amplitude of tensor and scalar perturbations. It is well known that an important limitation to the detectability of such peak comes from B-modes induced by gravitational lensing (Knox & Song 2002), especially on scales $\ell \gtrsim 100$. However, our analysis highlights that, at least for $\nu \lesssim 100$ GHz, B-modes produced by extragalactic radio sources are even more critical. A better understanding of polarization properties of dust in the Milky Way and in external galaxies is necessary to establish whether frequencies higher than 100 GHz may be more suitable to investigate the B-mode polarization.

Acknowledgements. We gratefully acknowledge the financial support provided through the European Community's Human Potential Programme under contract HPRN-CT-2000-00124, CMBNET, and through the Spanish Ministerio de Ciencia y Tecnología, reference ESP2002-04141-C03-01. GDZ has been partially supported by ASI and MIUR (COFIN 2002).

REFERENCES

Aller M. F., Aller H. D., Hughes P. A., 1992, *ApJ*, 399, 16.
 Aller M. F., Aller H. D., Hughes P. A., Latimer G. E., 1999, *ApJ*, 512, 601.
 Baccigalupi C., Burigana C., Perrotta F., De Zotti G., La Porta L., Maino D., Maris M., Paladini R., 2001, *A&A*, 372, 8.
 Barkats D., 2003, in *The Cosmic Microwave Background and its Polarization*, Hanany S., Olive K.A. (eds.), New Astronomy Reviews, 47, 1077.
 Bennett C. L., Lawrence C. R., Burke B. F., Hewitt J. N., Mahoney J., 1986, *ApJS*, 61, 1.
 Bennett C. L., et al., 2003a, *ApJ*, 583, 1.
 Bennett C. L., et al., 2003b, *ApJS*, 148, 97.
 Benoit A., et al., 2003, *A&A*, submitted, astro-ph/0306222.
 Bruscoli M., Tucci M., Natale V., Carretti E., Fabbri R., Sbarra C., Cortiglioni S., 2002, *NewA*, 7, 171.
 Carretti E., et al., 2003, in *Polarimetry in Astronomy*, Fineschi S. (eds.), SPIE Symposium on Astronomical Telescopes and Instrumentation, Waikoloa, Hawaii, SPIE Conf. Proc. 4843, 305; astro-ph/0212067.
 Cecchini S., Cortiglioni S., Sault R., Sbarra C. (eds.), 2002, *Astrophysical Polarized Backgrounds*, AIP Conf. Proc. 609.
 Condon J. J., Cotton W. D., Greisen E. W., Yin Q. F., Perley R. A., Taylor G. B., Broderick J. J., 1998, *AJ*, 115, 1693.
 De Zotti G., Gruppioni C., Ciliegi P., Burigana C., Danese L., 1999, *NewA*, 4, 481.
 De Zotti G., Granato G.L., Silva L., Maino D., Danese L., 2000, *A&A*, 354, 467.
 Eichendorf W., Reinhardt M., 1979, *Ap&SS*, 61, 153.
 Farese P.C., et al., 2003, in *The Cosmic Microwave Background and its Polarization*, Hanany S., Olive K.A. (eds.), New Astronomy Reviews, 47, 1033.
 Fosalba P., Lazarian A., Prunet S., Tauber J. A., 2002, *ApJ*, 564, 762.
 Gregory P. C., Scott W. K., Douglas K., Condon J. J., 1996, *ApJS*, 103, 427.
 Griffith M., Langston G., Heflin M., Conner S., Lehar J., Burke B., 1990, *ApJS*, 74, 129.
 Griffith M., Heflin M., Conner S., Burke B., Langston G., 1991, *ApJS*, 75, 801.
 Hanany S., Olive K.A. (eds.), 2003, *The Cosmic Microwave Background and its Polarization*, New Astronomy Reviews.
 Knox L., Song Y.-S., 2002, *Phys. Rev. Lett.*, 89, 011303.
 Kovac J. M., Leitch E. M., Pryke C., Carlstrom J. E., Halverson N. W., Holzapfel W. L., 2002, *Nature*, 420, 772.
 Kogut A., et al., 2003, *ApJS*, 148, 161.
 Kamionkowski M., Kosowsky A., Stebbins A., 1997, *Phys. Rev. D*, 55, 7368.
 Langston G. I., Heflin M. B., Conner S. R., Lehar J., Carrilli C. L., Burke B. F., 1990, *ApJS*, 72, 621.
 Lister M. L., 2001, *A&AS*, 198, 7908.
 Mason B.S., et al., 2003, *ApJ*, 591, 540.
 Mesa D., Baccigalupi C., De Zotti G., Gregorini L., Mack K.-H., Vigotti M., Klein U., 2002, *A&A*, 396, 463 (M02).
 Nartallo R., Gear W. K., Murray A. G., Robson E. I., Hough J. H., 1998, *MNRAS*, 297, 667.
 O'Dea C.P., 1989, *A&A*, 210, 35.
 O'Dea C.P., Baum S.A., Stanghellini C., Morris G.B., Patnaik A.R., Gopal-Krishna, 1990, *A&ASS*, 84, 549.
 Okudaira A., Tabara H., Kato T., Inoue M., 1993, *PASJ*, 45, 153.
 Pentericci L., Van Reeven W., Carilli C.L., Rötgering H.J.A., Miley G.K., 2000, *A&AS*, 145, 121.
 Perley R. A., 1982, *AJ*, 87, 6.
 Pearson T.J., Readhead A.C.S., 1981, *ApJ*, 248, 61.
 Pearson T.J., Readhead A.C.S., 1988, *ApJ*, 328, 114.
 Prunet S., Sethi S. K., Bouchet F. R., Miville-Deschénes M.A., 1998, *A&A*, 339, 187.
 Ricci R., Prandoni I., Gruppioni C., Sault R.J., De Zotti G., 2003, *A&A*, accepted; astro-ph/0312163.
 Rudnick L., Jones T. W., Aller H. D., Aller M. F., Hodge P. E., Owen F. N., Fiedler R. L., Puschell J. J., Bignell R. C., 1985, *ApJS*, 57, 693.
 Seljak U., 1997, *ApJ*, 482, 6.
 Seljak U., Zaldarriaga M., 1996, *ApJ*, 469, 437.
 Simard-Normandin M., Kronberg P. P., Button S., 1981, *ApJS*, 45, 97.
 Stanghellini, C., 1999, *Mem. SAIt*, 70, 117.
 Stanghellini C., O'Dea C. P., Dallacasa D., Baum S. A., Fanti R., Fanti C., 1998, *A&AS*, 131, 303.

Tabara H., Inoue M., 1980, A&AS, 39, 379.
 Taylor G. B., 2000, ApJ, 533, 95.
 Taylor A.C., Grainge K., Jones M. E., Pooley G. G., Saunders R. D. E., Waldram E. M., 2001, MNRAS, 327, L1.
 Tegmark M., Efstathiou G., 1996, MNRAS, 281, 1297.
 Toffolatti L., Argüeso-Gomez F., De Zotti G., Mazzei P., Franceschini L., Danese L., Burigana C., 1998, MNRAS, 297, 117 (T98).
 Toffolatti L., et al., 2003, in preparation.
 Trushkin, S.A., 2003, Bull. Spec. Astrophys. Obs. N. Caucasus, 55, 90; astro-ph/0307205.
 Tucci M., Carretti E., Cecchini S., Fabbri R., Orsini M., Pierpaoli E., 2000, NewA, 5, 181.
 Tucci M., Carretti E., Cecchini S., Nicastro L., Fabbri R., Gaensler B.M., Dickey J.M., McClure-Griffiths N.M., 2002, ApJ, 579, 607.
 Vielva P., Martínez-González E., Gallegos J.E., Toffolatti L., Sanz J.L., 2003, MNRAS, 344, 89.
 Waldram E.M., Pooley G.G., Grainge K.J.B., Jones M.E., Saunders R.D.E., Scott P.F., Taylor A.C., 2003, MNRAS, 342, 915.
 Zaldarriaga M., Seljak U., 1997, Phys. Rev. D, 55, 1830.
 Zaldarriaga M., Seljak U., 1998, Phys. Rev. D, 58, 3003.
 Zukowski E. L., Kronberg P. P., Forkert T., Wielebinski R., 1999, A&AS, 135, 571.